Proceedings of Ecos 2021 – The 34th International Conference On
Efficiency, Cost, Optimization, Simulation and Environmental Impact of Energy Systems
June 27-July 2, 2021, Taormina, Italy

Renewable Energy Based Systems with Heat Pumps for Supplying Heating and Cooling in Residential Buildings

Marika Pilou[a], George Kosmadakis[b], George Meramveliotakis[c] and Achileas Krikas[d]

Thermal Hydraulics and Multiphase Flow Laboratory, INRaSTES, National Centre for Scientific Research "Demokritos", Agia Paraskevi, Greece
[a] pilou@ipta.demokritos.gr
[b] gkosmad@ipta.demokritos.gr *(CA)*
[c] gmera@ipta.demokritos.gr
[d] a.krikas@ipta.demokritos.gr

Abstract:

An innovative configuration of an energy system for residential buildings is examined, with the use of a numerical tool that has been developed for simulating renewable energy-based systems based on geothermal and solar energy. The main components are the PV-Thermal (PVT) collectors and a multi-source heat pump supplied by heat from either the ambient air or water, with the option to include a borehole thermal energy storage (BTES) field to increase the system's overall efficiency. In addition, there are three water tanks for short-term thermal energy storage; a main water tank for domestic hot water (DHW) production, and two buffer tanks, with one connected to the PVT, which supplies the heat pump (solar-assisted mode), and a second one that is charged by the heat pump and from which space heating/cooling is delivered to the building. The developed code in Python solves the non-linear system of equations derived by the mathematical description of these components and their connections for the temporal variations of the temperature in the tanks and the inlet/outlet of each component. The numerical tool is used for detailed investigation of the system performance over time, as well as for analysing various layouts. In the current work, focus is given on the positive effect of the BTES component in the energy system of a building in a warm climate (Athens, Greece) and in a cold one (Copenhagen, Denmark). As expected, PVT collectors contribute heat for DHW production mostly during summer in both locations, whereas during winter they mostly charge the solar buffer tank. Moreover, the improvement of COP for cooling production with BTES is especially prominent during summer in Athens, whereas the effect of the BTES becomes more important during winter in Copenhagen, where the heating demand is high.

Keywords:

Multi-source heat pump; borehole thermal energy storage; PVT collectors; residential buildings; Cooling and heating demand; Domestic hot water.

1. Introduction

Solar energy applications in buildings are increasing with many of them based on solar thermal collectors, photovoltaic (PV) panels or, in more advanced systems, hybrid photovoltaic-thermal (PVT) collectors [1]. At the same time, the use of domestic heat pumps for heating and cooling is rising [2], because of their capacity to meet the buildings' energy demand and reduce the final energy consumption, especially when they are supplied with low-temperature heat from a water flow instead of ambient air that greatly increases their performance [3].

The integration of the above two energy systems, i.e. solar-assisted heat pumps (SAHPs), results in maximum solar energy utilization during the year and enhances the performance of the individual components [4]. The main functionality of such integrated approach is to either provide the required heat to the users directly from the solar collectors when the temperature is high enough or supply the heat pump with heat at low-temperature to increase its coefficient of performance (COP). A wide variety of thermal coupling methods exists, such as with direct or indirect heat transfer from the collector, aiming to improve the combined efficiency. Another concept that does not rely on the solar-assistance principle is the PV plus heat pump, which requires less piping and connections [5], with the focus being placed on reducing the electricity consumption from the grid and the maximization of self-consumption. However, the use of solar energy components come with a high

intermittency, with the produced heat or electricity showing large variations during the day and season, facing a challenge on reducing the annual energy consumption.

To resolve this, geothermal energy is often used as a supplementary renewable energy source, since the ground temperature shows minor fluctuations during the year, which are balanced to some extent by extracting heat in winter and rejecting heat during summer, where applicable [3]. The integration of solar and geothermal energy then offers a high flexibility to adjust the system operation and exploit the source that enhances the heat pump performance for both heating and cooling production. Relevant to this, several configurations have been proposed for building energy systems [6], revealing that further research is needed to better evaluate such integration.

Based on the above general principles of combining either solar thermal collectors or PV panels with heat pumps, an alternative design is proposed here, based on the use of PVT collectors that produce simultaneously heat and electricity [7]. In such a coupling, the high-temperature heat production by the PVT is used to cover DHW or space heating demand, whereas the low-temperature heat supplies the heat pump. The evaporation pressure in this case is increased, thus the heat pump COP improves significantly [8]. Moreover, a multi-source heat pump is at the core of the suggested configuration that is supplied with heat from either the ambient air or water, with the selection based on the maximum performance, with the option to include a borehole thermal energy storage (BTES) field to further increase the system's overall efficiency. The system includes standard (low-cost) water tanks to supply domestic hot water (DHW) and to store heating or cooling to cover the energy demand of the building, to introduce operational flexibility by decoupling production and consumption up to some extent. It should be stressed that the techno-economic evaluation of such concept is not within the scope of the current work, which focuses mostly on the performance indicators of such integrated system.

The main components of the integrated energy system under study are described in Section 2, along with their mathematical representation, whereas section 3 outlines the numerical tool with its inputs and parameters. Section 4 presents the system operation and performance for a multi-family residential building located in Athens (Greece) and Copenhagen (Denmark), considering several parameters, such as PVT surface area, heating/cooling demand profiles, , while giving emphasis on the positive effects of the BTES component. Finally, the conclusions of this study and the further steps are highlighted in Section 5.

2. Energy system based on solar and geothermal energy

2.1. System overview

The main system components are the PVT collectors for producing heat and electricity and the multi-source electric-driven heat pump. The system is intended to cover the space heating/cooling and DHW demand of a multi-family residential building. Two main layouts are examined, with or without the use of a BTES, while both include three water tanks. The heating and cooling modes of the system layout with BTES are illustrated in Fig. 1, along with the main system components and their connections with the possible options for selecting the heat source and heat sink.

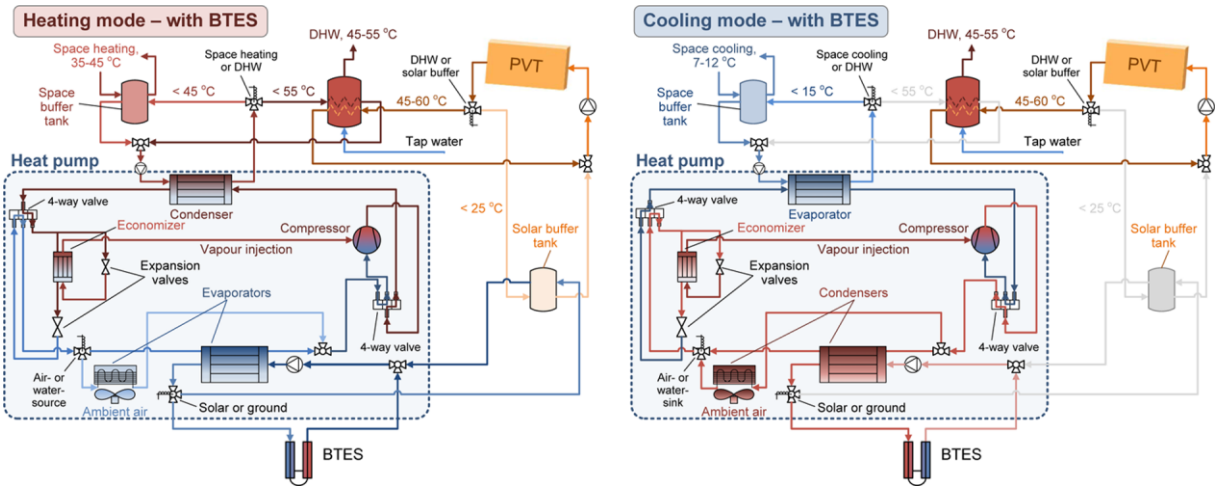

Fig. 1 System layout with the PVT collectors, the multi-source heat pump (blue shaded box), the BTES and the three water tanks. Left: Heating mode, Right: Cooling mode.

2.1.1. Heating mode

At moments with high solar irradiation, the heat produced by the PVT collectors charges the main water tank that is used for covering the building's DHW needs. Otherwise when the solar radiation is low, the produced heat is stored in another tank (the so-called "solar buffer tank"), which is kept at a lower temperature and is

used as a heat source to the evaporator of the heat pump, which then charges the main tank for DHW at up to 55°C or the space buffer tank for space heating at up to 45°C. The latter stores heat that is supplied to the building for covering its space heating demand, and its use enhances the system flexibility, by decoupling to some extent the time of heating demand with the heat pump operation, with an overall aim to reduce the electricity demand from the grid.

There are three options for the heat source of the heat pump, selecting the one that maximizes the COP: (1) water-source from the BTES, (2) water-source from the solar buffer tank, and (3) air-source from the ambient. In case no BTES is included in the system configuration, the options are limited to two. The most efficient is to operate at water-source mode, with the selection based on the highest temperature of either the BTES or the solar buffer tank. The air-source is only selected, when the ambient temperature is about 7°C higher than the water temperature, which takes place only during summer season mostly for DHW production.

2.1.2. Cooling mode

During the cooling mode in summer season, the space buffer tank is charged with cold water at a minimum temperature of about 7°C for delivering space cooling to the building. This is accomplished by reversing the heat pump operation with the use of two 4-way valves, while no simultaneous production of DHW and space cooling is possible, always giving priority to the DHW. Options similar to heating mode apply to the selection of the heat-sink of the heat pump for rejecting heat to: (1) the BTES, or (2) the ambient air. In case the system configuration does not include a BTES field, heat is always rejected to the ambient air.

2.2. Main system components

2.2.1. Heat pump

The heat pump includes an economizer with vapour injection for increasing the heating capacity and performance. The refrigerant selected is R1234ze(E), which is a hydrofluoroolefin (HFO) with ultra-low global warming potential (GWP) and a zero-ozone depletion potential (ODP). The modelling of the heat pump is based on a validated thermodynamic model developed in EES software [9], which follows a detailed approach for the cycle operation, considering a variable pinch-point temperature difference in all heat exchangers (HEXs) based on the initial sizing, and pressure drop at the different parts of the cycle. The model has been enriched here to account for: (1) the finned-tube heat exchanger (HEX) for the air-source operation, and (2) the compressor model. In the latter the volumetric and isentropic efficiency has been introduced as a function of volume flow rates at the inlet and outlet of the compressor, based on a semi-hermetic screw compressor of Bitzer with a displacement of 140 m^3/h at 50 Hz, resulting to a maximum heating capacity of about 100 kW. The COP for heating is then expressed as the ratio of the heating production to the electricity consumption, while for cooling it is the ratio of cooling production divided to the electricity. Depending on how the COP is expressed, there are two approaches, given next: (1) heat pump COP, which considers only the electricity of the compressor, and (2) system COP, which considers the total electricity of the heat pump system including the inverter losses, and the consumption of the two water pumps and the air-fan (in case of air-source operation).

Various simulation runs have been conducted leading to the sizing of the main components (e.g., the plate HEXs, air-fan). Once sizing was specified, the heat pump operation has been examined for variable heat source and sink temperatures. The results have been processed and used in a regression analysis for developing polynomial correlations of the key parameters, COP and heating/cooling production as a function of the hot and cold side temperatures to allow a straightforward integration in the overall system model. In total, four different sets of correlations have been produced for heating with water or air, and cooling with water or air, which are provided in the Appendix.

2.2.2. PVT collector

The PVT collector features an asymmetric low-concentration stationary reflector design, with a total size of 2.31 × 0.955 m. The thermal and electrical capacity is 1250 and 250 W respectively at standard conditions. The heat gain per m^2 of the collector is given by Eq. (1).

$$P_{th} = n_{th,b} \cdot I_{b,T} \cdot IAM_{th} + n_{th,d} \cdot \left(I_{d,T} + I_{ref,T}\right) - \left[a_{th,1} \cdot (T_M - T_{amb}) + a_{th,2} \cdot (T_M - T_{amb})^2\right]$$

$$= \dot{m}_{PVT}\, c_{p,PVT} \left(T_{PVT,out} - T_{PVT,in}\right)/A, \qquad (1)$$

where $I_{b,T}$, $I_{d,T}$ and $I_{ref,T}$ are the hourly beam (direct), diffuse and reflective radiation components on the tilted collector surface, respectively, available by Trnsys software, given the location, azimuth angle and slope of the collector, IAM_{th} is the thermal incidence angle modifier, T_M is the mean water temperature in the PVT collector, T_{amb} is the ambient temperature, $\dot{m}_{PVT}$ is the mass flow rate of the water/glycol mixture, $c_{p,PVT}$ is its

specific heat capacity, $T_{PVT,out}$, $T_{PVT,in}$ are the outlet and inlet fluid temperatures from the collector respectively, and A is the total PVT collector surface.

The water/glycol mixture circulating in the PVT circuit has a high concentration of glycol of 40% by vol. with anticorrosive additives to protect the aluminium receiver of the PVT collector. The mixture properties (density and specific heat capacity) are given as a function of concentration and temperature from the available dataset provided by the manufacturer [10].

The thermal efficiency coefficients $n_{th,b}$ and $n_{th,d}$ correspond to heat acquisition by beam and diffuse irradiation, respectively. These coefficients and the thermal loss parameters $a_{th,1}$ and $a_{th,2}$ are characteristic of the collector and are given in Table 1.

Table 1. PVT collector – Efficiency parameters.

Parameter	Value	Units	Parameter	Value	Units
$n_{th,b}$	0.581	-	$n_{el,b}$	0.101	-
$n_{th,d}$	0.430	-	$n_{el,d}$	0.075	-
$a_{th,1}$	3.78	$W \cdot m^{-2} \cdot K^{-1}$	a_{el}	0.00336	K^{-1}
$a_{th,2}$	0.014	$W \cdot m^{-2} \cdot K^{-1}$			

The electrical production per m^2 of the PVT collector is given by Eq. (2).

$$P_{el} = \left[n_{el,b} \cdot I_{b,T} \cdot IAM_{el} + n_{el,d} \cdot \left(I_{d,T} + I_{ref,T}\right)\right] \cdot [1 - a_{el} \cdot (T_M - T_{stc})], \quad (2)$$

where T_{stc} is the standard temperature at test conditions equal to 25 ^{o}C, $n_{el,b}$ and $n_{el,d}$ are the electrical efficiency coefficients that correspond to electrical production by beam and diffuse irradiation, respectively, and a_{el} is the temperature loss coefficient, given in Table 1, and IAM_{el} is the electrical incidence angle modifier.

Further details of the collector with its performance parameters and modelling features are provided in Refs. [11,12].

2.2.3. Borehole thermal energy storage

The dynamics of the ground heat exchanger are based on a first-order response model, which is given by Eq. (3) [13].

$$M_g \cdot c_{p,g} \cdot \frac{dT_g}{dt} = \lambda'_g \left(T_\infty - T_g\right) - Q, \quad (3)$$

where M_g is the ground mass depending on the borehole depth, radius and number, $c_{p,g}$ is the ground specific heat capacity, T_g is the ground temperature and Q is the thermal power provided by the ground during winter or rejected to the ground during summer (equal to the evaporator or condenser heat respectively). In Eq.(3), $\lambda_g^{'} = \lambda_g \cdot L_g$, where λ_g is the ground thermal conductivity and L_g the total length of the ground heat exchanger, while T_∞ is the undisturbed ground temperature [14] given as a function of the borehole depth and the day of the year for a specific field.

The typical values that have been used to describe the main specifications of the BTES field are given in Table 2, based on double U-pipes [15].

Table 2. BTES field characteristics

Parameter	Value	Unit
Borehole radius (r_b)	0.09	m
Ground density (ρ_g)	2500	$kg \cdot m^{-3}$
Borehole depth (L_b)	80	m
Ground specific heat capacity ($c_{p,g}$)	0.8	$kJ \cdot kg^{-1} \cdot K^{-1}$
Ground thermal conductivity (λ_g)	2	$W \cdot kg^{-1} \cdot K^{-1}$

The undisturbed ground temperature depends on the mean surface temperature, T_m, and its amplitude, A_s, are extracted from the PVGIS tool [16]. For the two locations that are examined here, Athens (Greece) and Copenhagen (Denmark), the mean surface temperature is 18^{o}C in Athens and 9.4^{o}C in Copenhagen, whereas the amplitude of the surface temperature is 7.2^{o}C in Athens, and 8.9^{o}C in Copenhagen. The number of the boreholes for a given installation is usually selected based on the required heating/cooling capacity of the system. Therefore, the system configuration in Athens includes 16 boreholes, while their number increases to 24 in Copenhagen due to the higher space heating demand, all with a depth of 80 m.

2.2.4. Water tanks

The energy system includes two different types of water tanks, namely the main water tank and the buffer water tank (Fig. 1). The main water tank (MWT) is supplied with heat directly from the PVT collectors for hot water production. The heat pump acts as an auxiliary heat source to the MWT, if the heat delivered from the PVT is not enough. There are high temperature differences between the bottom and top areas of the tank, thus stratification is needed to maximize thermal energy storage [17]. The MWT is of hybrid type, i.e. heat is delivered from the PVT and the heat pump through immersed heat exchangers, whereas tap water flows from the bottom of the tank to its top. The main water tank is modelled by splitting the tank in a finite number of 1-D volumes across the axis of equal height and applying energy balance in each volume [18]. Heat transfer occurs between the volumes and between the volumes and the immersed heat exchangers. Ambient heat losses are calculated from each volume separately, according to its temperature and surface in contact with the tank walls. The inverse temperature problem is treated here by artificially increasing the thermal conductivity between two adjacent volumes [19]. A constant multiplication factor equal to 10000 has been used to increase heat transfer by conduction once a volume temperature is higher than its upper volume. This approach was found to effectively eliminate this problem and capture experimental and empirical observations.

There are two buffer water tanks (BWT) incorporated in the system, as described previously. The limited temperature range of the BWTs, usually by about ±10^{o}C, with a small variation between the inlet/outlet temperature of the water flows, renders the assumption of uniform temperature within the whole tank valid (single-volume model) [18]. The BWT temperature is calculated by solving the unsteady energy balance equation, which incorporates terms for heat source and sink, as well as for the heat losses to the ambient.

3. Numerical Tool

3.1. General overview

The numerical tool in Python was developed to solve the system of equations for all components of a buildings' energy system, which are described in Section 2. The program consists of three main parts: pre-processing, calculation, and post-processing. At pre-processing a variety of input data are read and then several constant quantities (parameters) are set. Also, the initial values of the unknown variables are defined and based on them initial values of time-dependent parameters and flags are set. These flags are related to the system operation; they switch on/off the various components and/or redirect the flow to charge the different tanks as needed. Next, the main part of the program begins, where at each time-step the non-linear set of equations of the unknowns are defined depending on the operating status of the components in the specific time-step (time-step equal to 15 minutes) and solved for the temperatures and the time-dependent variables of all components. At the end of the simulation comes the post-processing, where a variety of additional quantities are calculated (power, efficiencies, stored thermal energy, COP, etc.). The tool was designed with flexibility in mind and allows for easy inclusion/exclusion of components, as well as components' equations.

3.2. Required Input

The numerical tool requires several parameters that describe the components sizing and operation, as well as input regarding local weather data and the building's energy demand. These are highlighted next.

3.2.1. Parameters

The parameters of the system are divided into two main categories: (1) sizing and (2) operational. The sizing parameters mainly concern the size/capacity of the system components and include for example the volume of the water tanks, the surface area of the PVT collectors, the borehole depth, number, and diameter and the number of apartments of the residential building. These have an impact on the system performance and the operational profile. Except from the sizing, the main specifications of the components are defined as well, e.g., the heat transfer coefficient of the outer tank wall (MWT, BWT), the concentration of glycol in the solar fluid, and the density, specific heat capacity and thermal conductivity of the ground.

The operational parameters are mostly introduced by the constraints imposed regarding the different components. For example, there is a prioritization in heat production by the heat pump, aligned with the user needs and this affects the operation of the heat pump. In this study, covering the DHW demand during both seasons is prioritized over keeping the space BWT warm (winter) or cool (summer) enough to provide to or absorb heat from the building, respectively. Moreover, the selection of the heat source at water-source operation is decided according to the one having the highest temperature available, air or water, and the latter involves further comparison between the solar BWT and the ground temperatures, when BTES is introduced to the system.

3.2.2. Weather data

The necessary weather data to perform the calculations have been obtained from Trnsys software [20], using the Type 109 component of this software, which reads the available TMY2 weather data for the 15-min time-step defined. The processed data include the solar radiation components on a tilted surface and angle of incidence with a fixed tilt of 30° and azimuth of 0°. For the simulations presented here, the TMY2 weather data for Athens and Copenhagen have been used to extract the necessary solar irradiation components (beam, diffuse and total), as well as the ambient temperature during the whole year.

3.2.3. Domestic Hot Water Demand

The DHW demand required by the model is calculated according to EN16147:2017 standard for water-heaters, hot water storage appliances and water heating systems [21]. The standard defines a 24h measurement tapping cycle with a draw temperature and flow rate leading to the calculation of the total thermal energy of 11.655 kWh per apartment and per day, corresponding to the "L" profile. However, an alternative approach is followed here [22], using as input the thermal energy for a hot water temperature of over 45°C and then calculating the flow rate. Based on this profile that is the same for every day of the year, the location specific DHW demand profile was then calculated which considers the annual temperature variation of the tap water in each location and the seasonal variability in hot water [20,22]. The monthly variation of DHW demand for a 5-apartment building is shown in Fig. 2(a) for Athens and Copenhagen. It should be noted that these profiles are obtained by assuming that the apartments' DHW demands do not overlap; one apartment follows the timeframe proposed by the "L" profile, while a positive or negative time shift is introduced for the demand of each subsequent apartment.

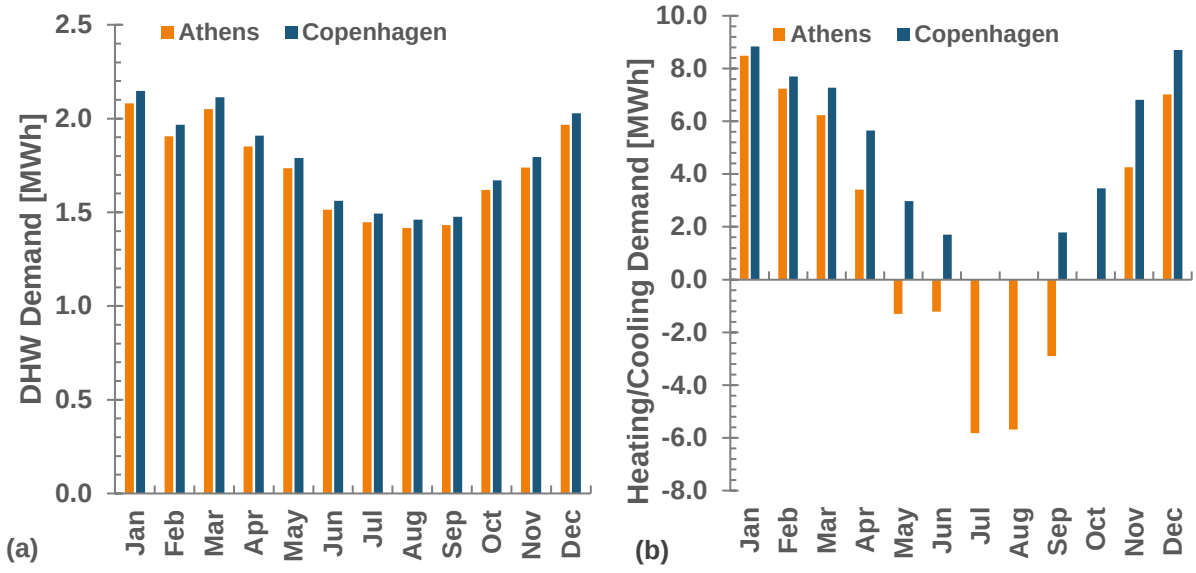

Fig. 2. Monthly 5-apartment building demands in Athens and Copenhagen: a) domestic hot water, and b) space heating/cooling – medium profile.

3.2.4. Space heating/cooling Demand

The space heating/cooling demand profile is estimated by an in-house code developed in Python exclusively for that purpose. The numerical methodology is based on thermal zones (one for each floor, for multi-family residential buildings), thermostat preferences, building specifications (e.g., surface area and U values of the walls), solar heat gains and internal gains from occupants [23,24]. A smart thermostat approach is introduced into the code, for restricting the sharp increase of space heating and cooling demand at peak hours, and thus smooth the profiles, indicating a realistic handling of the building loads. Furthermore, it is considered that the temperature in each floor is stabilized to a certain value when occupants are absent, based on typical occupancy profiles. Calculation of the necessary thermal loads to keep the indoor air temperature to the set-point temperature, allowing a variation of ±1 K, is based on distinguishing between heating and cooling seasons [25].

In this study, three profiles were generated for each location corresponding to low, medium, and high space heating/cooling demand, by adjusting the U values of the walls, roof and windows from 0.8 to 3 $W \cdot m^{-2} \cdot K^{-1}$ in Athens and from 0.6 to 1.6 $W \cdot m^{-2} \cdot K^{-1}$ in Copenhagen. These values are typical for old to new buildings in Greece and Denmark [26], resulting to a specific energy demand in the range of 56-157 $kWh \cdot m^{-2} \cdot year^{-1}$ in Athens (space cooling in the range of 26-42 $kWh \cdot m^{-2} \cdot year^{-1}$) and 57-164 $kWh \cdot m^{-2} \cdot year^{-1}$ in Copenhagen. The cumulative monthly space heating/cooling demand for Athens and Copenhagen that corresponds to the

medium demand for a 5-apartment building is shown in Fig. 2(b). It should be noted that due to the local weather conditions there is no need for cooling in Copenhagen.

3.3. Cases Examined

In the present study, the overall performance and efficiency of the system was numerically examined considering several key parameters for a 5-apartment building. In particular, for both locations, Athens (warm climate) and Copenhagen (cold climate), simulations were performed for the three space heating/cooling demand profiles, as well as for three PVT collectors surface areas of 50, 75 and 100 m^2. In all cases, the calculations were done for the same building energy system without and with BTES.

Special consideration was given to the sizing of the water tanks of the system. A parametric study examined the effect of the tank size on the system's annual electricity demand, with their volume ranging from 0.75 up to 3 m^3 in different combinations. This range corresponds to a specific tank volume from about 15 to 80 $l \cdot m^{-2}$ of collector surface. The processing of the results showed that a MWT of 2 m^3, a solar BWT of 1.5 m^3 and a space BWT of 3 m^3 yield the minimum annual electricity demand for systems with and without BTES, in both locations and all space demand profiles – PVT surface areas combinations. This tank sizing corresponds to a specific volume of 35-70 $l \cdot m^{-2}$, and has been used in all simulated cases with the results presented next.

4. Results and discussion

4.1. Daily operation

The main highlights of the system's daily operation are initially presented during a winter and summer day, in order to better understand the charging processes of the tanks. The charging is easily expressed through the water temperature evolution in the MWT during these two representatives days for the system with BTES in Athens, presented in Fig. 3, for all three space heating/cooling profiles and a PVT surface of 75 m^2. The MWT has been divided into two segments, the "Top" that includes the water volumes at the upper part of the tank that are supplied by the heat pump, and the "Bottom" supplied by the PVT.

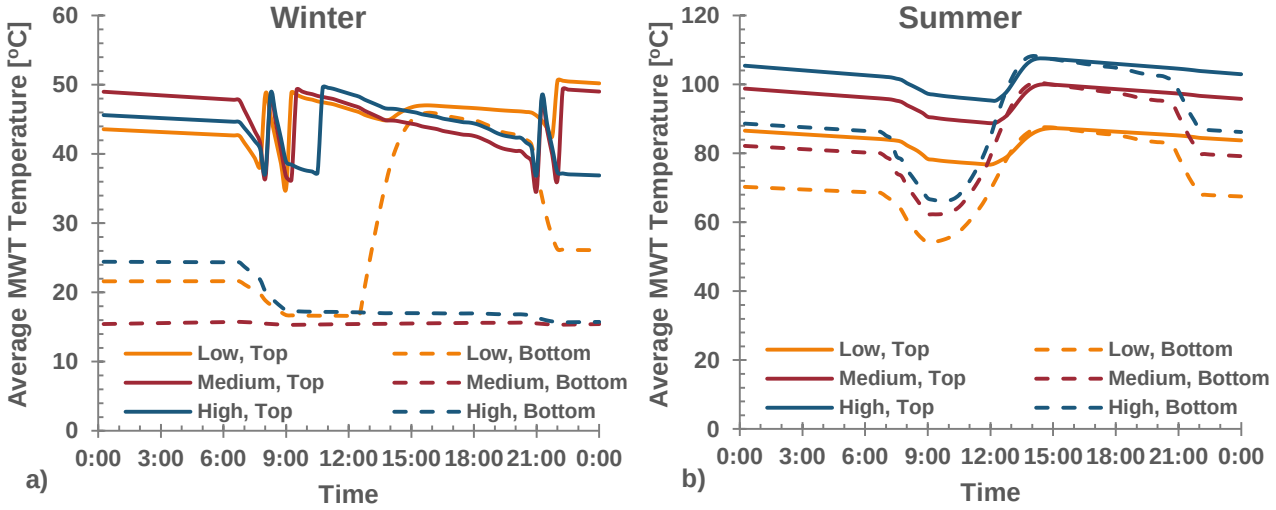

Fig. 3 Average MWT temperature over volumes supplied by the PVT (Bottom) and the heat pump (Top) for the three space heating/cooling profiles in Athens with BTES, during: a) winter day, and b) summer day

During the winter day, the moments that there is DHW demand is visible by sharp temperature drops in the "Top" curves mostly, with the heat pump operating for two periods during this day (early morning and evening).to keep a high enough temperature so that DHW is delivered at a temperature of over 45°C. The temperature at the bottom part of the MWT is considerably lower, and further decreases close to the tap water temperarure (~15°C), since the PVT collectors do not charge this tank during winter for most of the cases. Instead, the PVT charge the solar buffer tank, which is kept at a lower temperature (below 25°C). A large stratification is observed that favours the heat pump performance and reduces the electricity consumption for covering the DHW demand at all times.

During the summer day, the MWT is maintained at high temperatures of over 55°C throughout the day. The temperature drop at moments with a DHW demand is not sharp due to the large amounts of stored thermal energy by the PVT collectors, and the small slope of "Top" temperature rise after demand indicates that the top part of the MWT is reheated by the warmer water volumes that are at the bottom part of the tank, after solving the inverse temperature issue leading to the lost of any stratification. The heat pump does not operate during this day with all the DHW demand covered by the PVT collectors. It should be highlighted that the

elevated temperature in the tank is sufficient to cover the DHW demand of the next day as well. Main performance indicators are given in *Table 3* during a winter and a summer day that include system demands and supplies in heat and electricity, as well as the daily average COP. These indicators are related to both the heat pump and the PVT collectors with a surface of 75 m^2 for an energy system without and with BTES in Athens and Copenhagen for a building with the medium space heating/cooling profile. It should be stressed that the system COP indicator includes the electricity consumption of all auxiliaries related to the heat pump. If these are omitted, the COP increases on average by 0.2-0.3, becoming almost 5 in Athens during summer.

Additionally, electricity produced by the PVT during the winter day is 26% of the system demand in Athens, but only 1% in Copenhagen, due to the lower available solar irradiation. Nevertheless, during the summer day there is a surplus of electricity by the PVT in Copenhagen. It is noticeable that during the specific summer day in Copenhagen, there is no (without BTES) or limited (with BTES) supply of heat to the MWT to cover the building's demand for DHW, though the corresponding demand is not zero. Further inquiry into the model's daily results revealed that this is common in both cities during summertime, and appears after days (one or more consecutive) of the MWT being fully charged by the PVT. This leads to an increased water temperature in the tank, which, combined with the lower DHW demand in the summer, is sufficient to cover the demand, without the need for the heat pump to operate.

Table 3. Performance indicators during a winter and a summer day in Athens and Copenhagen, without and with BTES (A_{PVT} = 75 m^2, medium space heating/cooling profile).

	Athens				Copenhagen			
	Winter		Summer		Winter		Summer	
Daily indicators	w/o BTES	BTES	w/o BTES	BTES	w/o BTES	BTES	w/o BTES	BTES
Space Heating Demand [kWh]	239.8		-		286.6		-	
Space Cooling Demand [kWh]	-		119.2		-		0.0	
DHW demand [kWh]	67.6		46.3		69.7		47.7	
PVT heat to DHW [kWh]	50.2	0.0	69.4	69.4	0.0	0.0	0.0	0.0
PVT heat to solar BWT [kWh]	62.2	0.0	1.1	1.1	5.6	0.0	0.0	0.0
HP heat to DHW [kWh]	50.0	71.0	0.0	0.0	71.7	70.7	0.0	17.3
HP heat/cold to space BWT [kWh]	254.0	270.0	123.3	128.6	310.5	321.5	0.0	0.0
PVT electricity [kWh]	22.3	23.8	28.1	28.1	1.4	1.4	32.4	32.5
System electricity demand [kWh]	84.5	85.6	48.9	27.7	117.3	108.6	0.0	4.8
Average system COP [-]	3.6	4.0	2.5	4.6	3.3	3.6	n/a	3.6

The results show the effect of BTES in the overall operation of the system. For example, in winter in Athens, there is significant supply of heat by the PVT to both the MWT and the solar BWT when the system operates without BTES. However, the PVT heat contribution becomes zero when BTES is included, because the ground temperature is such that renders BTES favourable for heat pump supply against the solar BWT or the ambient (outdoor) air, with the buffer tank kept fully charged in both locations. In summer, the use of the BTES does not affect the PVT operation in both locations, which increases the system's daily average COP. This is especially obvious in Athens, where the space cooling demand is high, with the system COP increasing by 84%. It should be stressed that the system COP indicator includes the electricity consumption of all auxiliaries related to the heat pump. In case these are not included, the COP increases by about 0.2-0.3 in average, reaching almost 5 in Athens during summer.

Additionally, electricity produced by the PVT during the winter day is 26% of the system demand in Athens, but only 1% in Copenhagen, due to the lower available solar irradiation. Nevertheless, during the summer day there is a surplus of electricity by the PVT in Copenhagen. It is noticeable that during the specific summer day in Copenhagen, there is no (without BTES) or limited (with BTES) supply of heat to the MWT to cover the building's demand for DHW, though the corresponding demand is not zero. Further inquiry into the model's daily results revealed that this is common in both cities during summertime, and appears after days (one or more consecutive) of the MWT being fully charged by the PVT. This leads to an increased water temperature in the tank, which, combined with the lower DHW demand in the summer, is sufficient to cover the demand, without the need for the heat pump to operate.

4.2. Monthly operation

Next, the results are summed to provide the monthly performance. The monthly variation of the system COP is shown in Fig. 4 for Athens and Copenhagen, without and with BTES, in the case of PVT total surface area of 75 m^2 and medium space heating/cooling demand profile.

In Athens without BTES, the system COP is around 3.6 in months with space heating demand (Jan-Apr and Nov-Dec), with the heat pump operating for long periods at solar-assisted mode. The system COP drops to about 2.3 during the summer months due to the high space cooling demand, since the heat pump rejects heat to the ambient air with a reduced performance. The effect of BTES in raising the system COP is prominent between May and September in Athens, lifting the system COP to over 4.5. In Copenhagen on the other hand, the effect of BTES is significant during the colder months (high space heating demand), increasing the COP by about 15-20% compared to the case without BTES.

Further conclusions can be drawn, focusing on the electricity production by the PVT and the consumption of the system. The monthly variation of electricity supply (PVT) and system demand with BTES in Athens and Copenhagen is presented in Fig. 5 for a PVT surface of 75 m^2 and for the medium space heating/cooling demand profile.

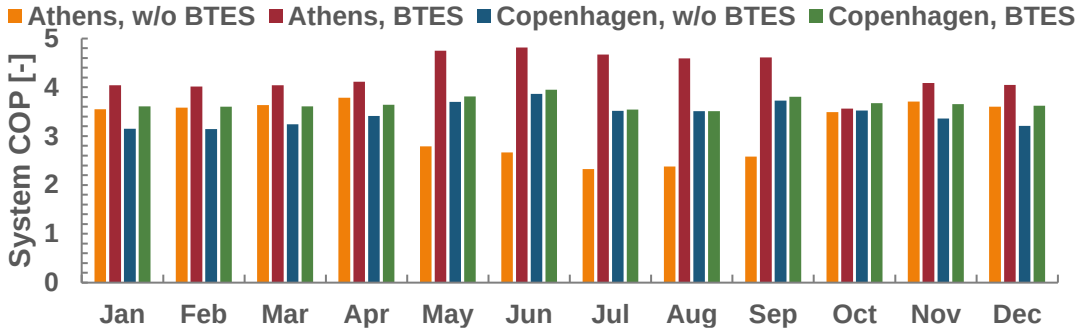

Fig. 4 Monthly variation of integrated system COP in Athens and Copenhagen without and with BTES (A_{PVT} = 75 m^2, medium space heating/cooling demand profile).

During the colder months (i.e. Jan-Mar and Nov-Dec for Athens, and Jan-Apr and Oct-Dec for Copenhagen), the PVT electricity production is considerably lower than the system demand; by 3-5 times for Athens, and by 3-26 times for Copenhagen. However, there are months during the summer period that PVT electricity can fully cover the system electricity demand. In Athens there is surplus of electricity by 2-4 times during May, June and September, but not for July and August, i.e. the months of maximum space cooling demand, where PVT electricity can cover about 70% of the demand. In Copenhagen, where there is no need for space cooling, there is a surplus of electricity by 1.5-7.5 times from June to August.

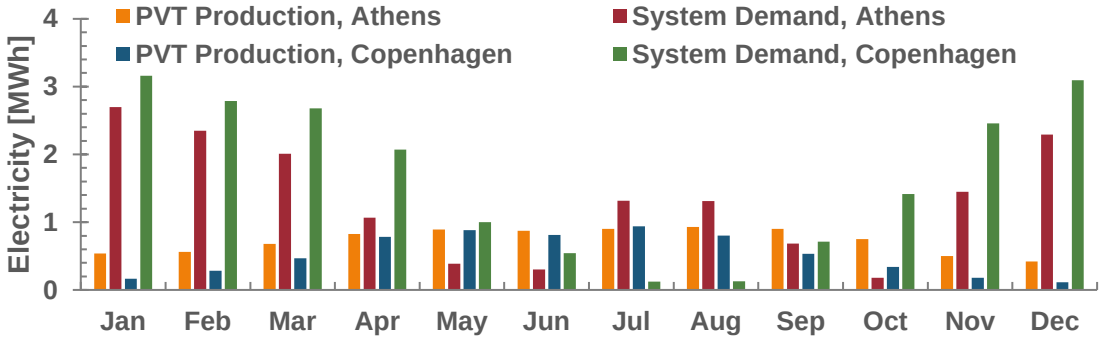

Fig. 5 Monthly electric energy demand and PVT production for Athens and Copenhagen with BTES (A_{PVT} = 75 m^2, medium space heating/cooling demand profile).

By increasing the PVT surface to 100 m^2 or more, the electricity production is increased, leading to large amounts of excess heat during summer and over-heating of the collectors and the tank, requiring a separate heat rejection unit to protect the whole installation.

4.3. Annual operation

With the use of a heat pump, the heating and cooling is electrified and therefore the annual electricity balance becomes important. This is highlighted in Fig. 6, where the effect of BTES on the annual variation of the system's electricity demand is shown for Athens and Copenhagen as a function of PVT total surface area and space heating/cooling demand profile.

As expected, increased space demands lead to increased electricity consumption, in all cases. Moreover, including BTES in the system results in a lower electricity consumption, with such effect being stronger in Athens, where there are significant space cooling needs during summertime. The total surface area of the PVT has a minor effect on the annual system electricity demand mostly with the system without BTES, because even the smaller PVT surface covers the DHW demand for several months during the year.

The ratio of the annual PVT electricity production to system electricity demand increases as the space heating/cooling demand decreases, as shown in Fig. 7 for a PVT surface area of 75 m^2.

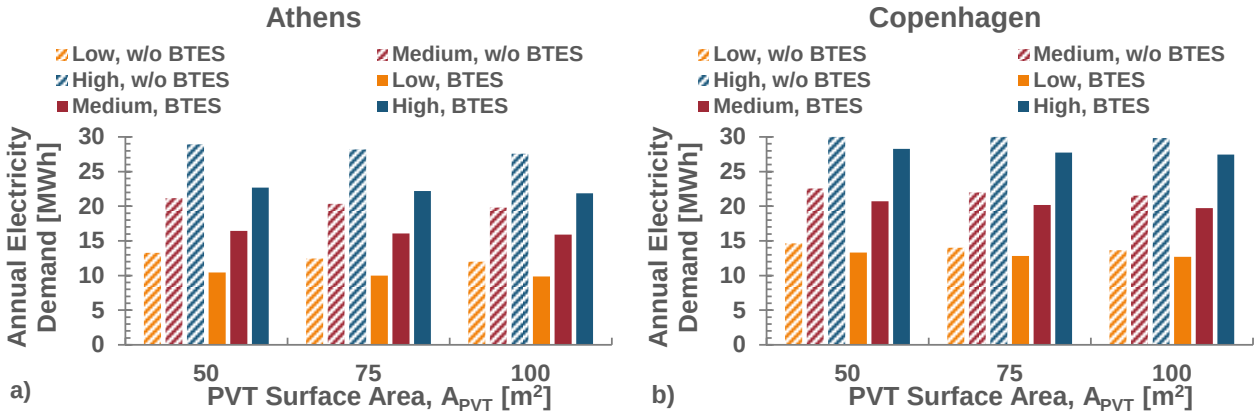

Fig. 6 Annual electricity demand vs. PVT surface area and space heating/cooling demand profiles, without and with BTES for: a) Athens, and b) Copenhagen

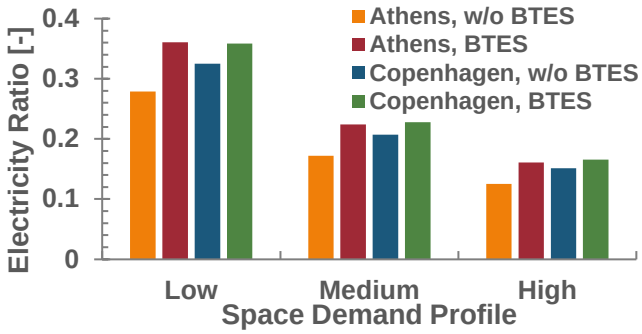

Fig. 7 Annual PVT electricity production to system demand ratio vs. space heating/cooling demand profiles for Athens and Copenhagen without and with BTES

For low space heating/cooling demand with BTES, electricity produced by the PVT can cover 36% and 33% of demand for Athens and Copenhagen, respectively on an annual basis. Including BTES in the energy system results in increased electricity ratio by about 23% for Athens, and by about 9% for Copenhagen. In addition, the simulations showed that increasing by 1/3 the PVT total surface area, i.e. from 75 to 100 m^2, leads to a proportional increase in the annual electricity ratio.

5. Conclusions and discussion

A renewable-based energy system for heating and cooling is proposed, with the multi-source heat pump being capable to select the source that maximizes its performance. By including BTES, the system flexibility increases especially at heating mode, since the heat pump is supplied by either heat from the ground, the solar buffer tank or the ambient air. Moreover, the PVT collectors produce both heat and electricity, with their heat production used directly for DHW production (charging the main water tank) or stored in a solar buffer tank. All three tanks have been sized so that the system consumes the lowest electricity.

The operation and performance of such system has been examined when considering the use of BTES or not, as well as for a variable PVT surface area and space heating/cooling demand profiles in a typical south European location (Athens, Greece) with significant space cooling demand during summer and in a northern one (Copenhagen, Denmark) with a high space heating demand during winter but no space cooling demand.

During winter, the use of BTES improves the heat pump COP and reduces the electricity consumption by up to 20% in both locations, assisted using the solar buffer tank that is charged by the PVT collectors, leading to a solar-assisted heat pump operation. However, the largest performance enhancement of BTES is observed during summer in Athens, since the space cooling demand is covered with a more efficient way, due to the low temperature lift of the heat pump (ground temperature of about 18-20 ºC, cooling delivery of 7 ºC). Moreover, the daily heat production of the PVT collectors is sufficient to cover the DHW demand during many summer days, but their production during winter is greatly reduced, especially in Copenhagen. The use of a larger total surface increases the electricity production but having a minor effect on the annual heat production. Therefore, their sizing is greatly decided from the maximum water temperature in the storage tanks in summer, in order to avoid over-heating and the rejection of the excess heat, which is also related to techno-economic aspects, not examined in the current work.

In terms of electricity balance, the system consumption is always higher than the PVT production on an annual basis, although the opposite applies in few months during summer in Copenhagen. Therefore, for reaching a net 100% renewable energy share it is necessary to include in the system configuration an electricity production component, with the use of standard PVs the most obvious one.

The next steps of this work are to introduce in the system layout an improved version of the PVT collector with an increased annual thermal and electric energy yield, as well as to expand the numerical algorithms towards the increase of self-consumption, which is possible due to the use of water storage tanks. After that, system variants will be also examined in other locations in Europe and for other building types, such as an office building, in which no DHW demand exists, requiring an alternative heat management strategy during summer, such as rejecting the PVT heat production to the ground.

Acknowledgments

This work has been performed within the RES4BUILD project (Renewables for clean energy buildings in a future power system) – Horizon 2020 program, Grant Agreement no. 814865.

Appendix

The heating capacity and COP of the heat pump for heating mode are given next, as a function of the inlet/outlet water temperature at the condenser and the inlet temperature at the evaporator. The range of validity is: outlet water temperature from the condenser ($T_{cd,out}$): 30-58 ^{o}C, inlet water temperature to the evaporator ($T_{ev,in}$): 4-28 ^{o}C, inlet air temperature to the evaporator ($T_{air,in}$): -15-30 ^{o}C.

Water-source

$$Q_{cd} = 5.60655200E+01 + 1.64593912E+00\,T_{ev,in} + 1.57141871E-02\,T_{ev,in}^2 + 3.22171655E-01\,T_{cd,out} - 1.17591400E-03\,T_{cd,out}^2 - 3.87666620E-03\,T_{ev,in}\,T_{cd,out}$$

$$COP_h = \frac{Q_{cd}}{P_{el}} = 1.00152090E+01 + 1.88170854E-01\,T_{ev,in} + 1.13775142E-03\,T_{ev,in}^2 - 2.35211344E-01 T_{cd,out} + 2.08733998E-03\,T_{cd,out}^2 - 3.28777520E-03\,T_{ev,in}\,T_{cd,out}$$

Air-source

$$Q_{cd} = 5.69203316E+01 + 1.01020670E+00\,T_{\mathrm{air},in} + 5.39703906E-03\,T_{\mathrm{air},in}^2 + 2.41415534E-01\,T_{cd,out} + 2.38757763E-03\,T_{cd,out}^2 + 1.37278409E-02\,T_{\mathrm{air},in}\,T_{cd,out}$$

$$COP_h = \frac{Q_{cd}}{P_{el}} = 8.79132713E+00 + 1.15357127E-01\,T_{air,in} + 1.92822711E-04\,T_{air,in}^2 - 1.65179359E-01\,T_{cd,out} + 1.16641805E-03\,T_{cd,out}^2 - 1.41567337E-03\,T_{air,in}\,T_{cd,out}$$

For cooling, the range of validity is: inlet water temperature to the condenser ($T_{cd,in}$): 15-26 ^{o}C, outlet water temperature to the evaporator ($T_{ev,out}$): 4-14 ^{o}C, inlet air temperature to the condenser ($T_{air,in}$): 20-40 ^{o}C.

Water-sink

$$Q_{ev} = 6.20507877E+01 + 2.31888309E+00T_{ev,out} + 3.05851097E-02T_{ev,out}^2 - 3.86757661E-01T_{cd,in} - 1.46533012E-03T_{cd,in}^2 - 1.90878948E-02T_{ev,out}T_{cd,in}$$

$$COP_c = \frac{Q_{ev}}{P_{el}} = 1.00787600E+01 - 4.32622654E-01T_{cd,in} + 7.13162134E-03 * T_{cd,in}^2 + 3.15462971E-01T_{ev,out} + 2.00489837E-03T_{ev,out}^2 - 9.45917886E-03 * T_{cd,in} * T_{ev,out}$$

Air-sink

$$Q_{ev} = 5.86676038E+01 + 2.46516804E+00T_{ev,out} + 1.97052912E-02T_{ev,out}^2 - 3.60089785E-01T_{air,in} - 2.61056062E-03*T_{air,in}^2 - 2.93270921E-02T_{ev,out}T_{air,in}$$

$$COP_c = \frac{Q_{ev}}{P_{el}} = 6.81258305E+00 - 2.14935806E-01T_{air,in} + 2.17281687E-03T_{air,in}^2 + 1.10421093E-01T_{ev,out} + 2.33429572E-07T_{ev,out}^2 - 2.32396085E-03 * T_{air,in} * T_{ev,out}$$

References

[1] Buker M.S., Riffat S.B., Solar assisted heat pump systems for low temperature water heating applications: A systematic review, Renew. Sustain. Energy Rev. 2016;55:399–413.

[2] Guo X., Goumba A.P., Air source heat pump for domestic hot water supply: Performance comparison between individual and building scale installations. Energy 2018;164:794–802.

[3] Naranjo-Mendoza C., Oyinlola M.A., Wright A.J., Greenough R.M., Experimental study of a domestic solar-assisted ground source heat pump with seasonal underground thermal energy storage through

shallow boreholes. Appl. Therm. Eng. 2019;162:114218.

[4] Kim T., Il Choi B., Han Y.S., Do K.H., A comparative investigation of solar-assisted heat pumps with solar thermal collectors for a hot water supply system. Energy Convers. Manag. 2018;172:472–484.

[5] Wang X., Xia L., Bales C., Zhang X., Copertaro B., Pan S., Wu J., A systematic review of recent air source heat pump (ASHP) systems assisted by solar thermal, photovoltaic and photovoltaic/thermal sources. Renew. Energy 2020;146:2472–2487.

[6] Nouri G., Noorollahi Y., Yousefi H., Solar assisted ground source heat pump systems – A review. Appl. Therm. Eng. 2019;163:114351.

[7] Vaishak S., Bhale P.V., Photovoltaic/thermal-solar assisted heat pump system: Current status and future prospects. Sol. Energy 2019;189:268–284.

[8] Fine J.P., Friedman J., Dworkin S.B., Detailed modeling of a novel photovoltaic thermal cascade heat pump domestic water heating system. Renew. Energy 2017;101: 500–513.

[9] Kosmadakis G., Arpagaus C., Neofytou P., Bertsch S., Techno-economic analysis of high-temperature heat pumps with low-global warming potential refrigerants for upgrading waste heat up to 150°C. Energy Convers. Manag. 2020;226:113488.

[10] Tyfocor, Tyfocor L technical information– Available at: <https://tyfo.de/downloads/TYFOCOR-L_en_TI.pdf>

[11] Gomes J., Diwan L., Bernardo R., Karlsson B., Minimizing the impact of shading at oblique solar angles in a fully enclosed asymmetric concentrating PVT collector. In: Energy Procedia, Elsevier Ltd, 2014:2176–2185.

[12] Ricardo B., Measurements of the Electrical Incidence Angle Modifiers of an Asymmetrical Photovoltaic/Thermal Compound Parabolic Concentrating-Collector. Engineering 2013;05:37–43.

[13] De Ridder F., Diehl M., Mulder G., Desmedt J., Van Bael J., An optimal control algorithm for borehole thermal energy storage systems. Energy Build. 2011;43:2918–2925.

[14] Labs K., The underground advantage: climate of soils, in: 4th Nat. Passiv. Sol. Conf., Am. Sect. ISES, 1979.

[15] Haller M., Dott R., Ruschenburg J., Ochs F., Bony J., A Technical Report of Subtask C Report C1 Part A. The Reference Framework for System Simulations of the IEA SHC Task 44/HPP Annex 38 Part A: General Simulation Boundary Conditions, 2013.

[16] EC-JRC, Photovoltaic Geographical Information System (PVGIS) – Available at: < https://re.jrc.ec.europa.eu/pvg_tools/en/>

[17] Rahman A., Smith A.D., Fumo N., Performance modeling and parametric study of a stratified water thermal storage tank, Appl. Therm. Eng. 2016;100:668–679.

[18] Panaras G., Mathioulakis E., Belessiotis V., Investigation of the performance of a combined solar thermal heat pump hot water system. Sol. Energy 2013;93:169–82.

[19] Cadafalch J., Carbonell D., Consul R., Ruiz R., Modelling of storage tanks with immersed heat exchangers. Sol. Energy 2015;112:154–162.

[20] Trnsys v. 16 software – Available at: <http://www.trnsys.com/>

[21] Directive 2009/125/EC of the European Parliament and of the Council with regard to ecodesign requirements for water heaters and hot water storage tanks, EU Regul. No 814/2013 2 August 2013 – Available at: <https://eur-lex.europa.eu/eli/reg/2013/814/2017-01-09>

[22] D' Antoni M., Fedrizzi R., Sparber W., Haller M., Solartechnik S., IEA-SHC Task 44 / HPP Annex 38, 2013.

[23] Hoogsteen G., Molderink A., Hurink J.L., Smit G.J.M., Generation of flexible domestic load profiles to evaluate Demand Side Management approaches. In: 2016 IEEE Int. Energy Conf. ENERGYCON 2016, Institute of Electrical and Electronics Engineers Inc., 2016 April 4-8; Leuven, Belgium.

[24] ASHRAE, ASHRAE Handbook. Fundamentals., SI edition, ASHRAE, USA, 2017.

[25] Meramveliotakis G., Kosmadakis G., Krikas A., Gomes J., Pilou M., Innovative Coupling of PVT Collectors with Electric-Driven Heat Pumps for Sustainable Buildings. In: EuroSun 2020 - 13th Int. Conf. Sol. Energy Build. Ind., 2020 Sep 1-3; Athens, Greece.

[26] TABULA WebTool2013 – Available at: <https://webtool.building-typology.eu>